Integrated system scanning probe microscope - quartz microbalance: *in-situ* testing of surface potential, topography and mass of the adsorbed gases.

V.S. Popov, R.G. Pavelko, A.V. Shelaev*, V.G. Sevastynov, N.T. Kuznetsov
N. S. Kurnakov Institute of General and Inorganic Chemistry, Russian Academy of Sciences, 119991, Leninskij prosp., 31, Moscow, Russia
** NT-MDT Co. 124482, Building 100, Zelenograd, Moscow, Russia*

Introduction

Integrated system of scanning probe microscopy (SPM) and quartz-crystal resonator (QCR) represent promising tool for *in-situ* measurement of electron work function change and the amount of the adsorbed analyte simultaneously. Separately, these techniques are very well studied and extensively used in the past decades. *In-situ* and *operando* study on the basis of Kelvin probe measurements on the working sensor were successfully applied by Barsan et. all and demonstrated huge potential of the technique in understanding surface processes related with gas sensor phenomenon [1]. On the other hand, piezoelectric microbalance is widely used technique for very precise mass detection, especially in the case of selective adsorption either from liquid or gas phase [2]. However, combination of these two methods seems to be not so much investigated, in spite of the fact that several publications are available in the literature. The integrated systems SPM/QMB, described so far, are mainly used for *in-situ* measurements of sample morphology and its mass, changing upon adsorption of the analyte [3-6].

The purpose of this study is to test integrated system SPM-QCR for *in-situ* measurements of surface potential and mass of the adsorbed target gases. As model systems we chose blank and palladium doped tin oxide, since these materials manifested remarkable sensitivity towards reducing gases [7], and hafnium oxide, coated with a bromocresol purple (BCP), which is promising material for detection of surface pH change upon analyte chemisorption [8]. 0.1 % hydrogen, 0.1 % methane and 10 % ammonia (all in air) were used as target gases in our experiments.

Experimental part

Integrated system of SPM/QCR

We used SPM Solver ProM (NT-MDT, Russia) with optical microscope integrated with QMB built-in gas-liquid cell MP3QCM (NT-MDT, Russia). Fig. 1 shows the design of the gas-liquid cell [9]. The cell consists of a carriage 1, base 2, bottom cell part 3 with build-in gold-coated spring contacts 4. Quartz-crystal resonator (QCR) 5 is placed on spring contacts. Fixation of the QCR is carried out by top cell part 6 with the nozzle 7 and by screw-nut 8. The gas is supplied through an input / output connectors 9. Tightness of the cell is provided by o-ring 10 between the upper and lower part, and a rubber membrane 11 between the probe holder and the upper part. AFM probe 13 is fixed in the probe holder, which allows you to apply electric DC and AC voltage to the probe.

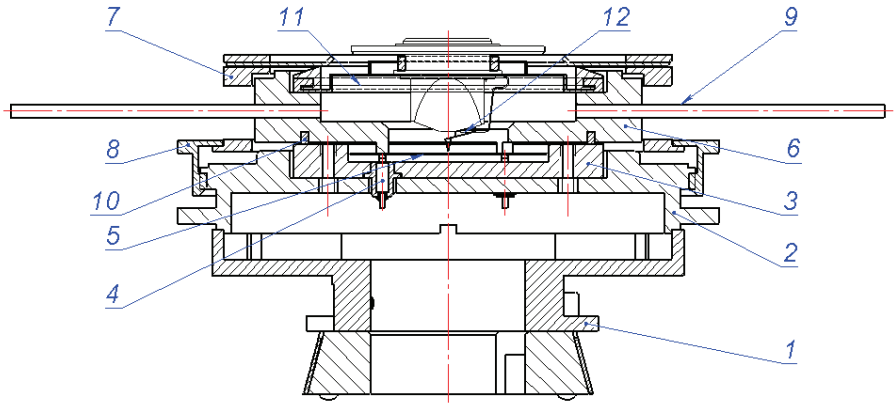

Fig. 1. Gas-liquid cell with integrated quartz microbalance.

Operation procedure is as follows. QCR with deposited sample material on the upper electrode is placed on the spring contacts in such a way that the upper electrode is grounded. Then top cell part is installed onto the base by the nozzle and screw-nut. The probe is installed in the probe holder which is mounted on a XYZ scanner. Membrane is fixed by clamping mechanism in the top cell part. One aligns AFM registration system and then AFM probe approached to the sample surface by step motor. After approach finished one can move carriage in XY direction to find required area on the surface and then scans the sample surface in contact or tapping technique including Kelvin probe. Gas could be supplied through the gas connectors.

The driving voltage is applied to quartz and its response is detected by controller, connected to the resonator by the spring contacts and coaxial cable. Parasitic capacitance is compensated by calibration procedure. Controller allows producing real-time measurements of the resonant frequency and Q-factor of the circuit. Detection of the resonator parameters could be produced simultaneously with the AFM measurements as well as separately. The accuracy of measuring the fundamental frequency is 0.04 Hz. Repeatability of the fundamental frequency after removal and installation of the QCR is +/- 1 Hz. For the 5 MHz quartz crystal the controller can excite vibrations in the higher harmonics up to 21th.

The relationship between the change of the QCR frequency and the change of the mass can be found from the Sauerbrey model [10]:

$$\Delta F = -2,3 \cdot 10^{6} \cdot F_0^2 \cdot \frac{\Delta m}{s} \qquad (1)$$

where ΔF - change the oscillation frequency of quartz resonator at the fundamental harmonic, Hz; F_0 – the natural frequency of vibration of the QCR, in MHz; Δm – mass change of the QCR, in g; s – area of the oscillating part of the QCR (between contacts), in cm^2.For the resonators used in this study (DM-6, NPF “Etna”, Russia) F_0 and s were equal to 5 MHz and 0.5 cm^2, respectively. And since the measurements were made at the third harmonic (15 MHz), the measured oscillation frequency $\Delta F`=3\cdot\Delta F$.

Substitution in (1) the specified values (i.e. F_0, s *and* ΔF) allows us to estimate the change of the sample mass as a function of the change in frequency:

$$\Delta m = -2,9 \cdot 10^{-9} \cdot \Delta F' \qquad (2)$$

From this relationship the experimental accuracy of the method amounts to 0.3 ng (ca. 10^{14} H_2 molecules).

The cantilever, used for the measurements, represented conductive silicon with boron doping probe DCP11 (NT-MDT, Russia). The probe has a protective diamond coating that avoids mechanical

damage of the cantilever tip due to its abrasion in contact with the sample. This will reduce the measurement error of the surface potential [11].

Measurements of surface properties of the sample were performed by scanning the sample surface in the two-pass mode technique. This allows one not only to image the surface topography of the sample in the semicontact mode, but also to map the distribution of surface potential with compensation of topography. The time needed for one scan is 10 min. Instrument accuracy of the surface potential measurements for the equipment configuration in question is 0.1 mV.

Gas-mixing and gas supply to the gas-liquid cell was realized using two mass flow controllers (EL-Flow, Bronkhorst), connected to the gas-liquid cell and gas cylinders. Synthetic air, and gas mixtures of 0.1 % hydrogen, 0.1 % methane and 10 % ammonia (all in air) were used to purge the cell until the mass equilibrium on the QCR is reached. Then surface potential and topography were scanned at room temperature.

Sample Preparation

Three materials were used in our experiments: blank SnO_2, SnO_2 doped with Pd and HfO_2 doped with BCP. All materials were deposited on the front side of the QCR DM-6, representing flat gold electrode on polished quartz membrane. Synthesis of blank SnO_2 (SnO_2) was realized directly onto the surface of QCR through thermal decomposition of tin acetate at 350 °C for one hour. SnO_2 doped with Pd (SnO_2-Pd) was synthesized previously according to [7]. The powder was dispersed in ethanol and the resulting colloid was deposited on the surface of QCR and dried at 350 °C for one hour. The third sample HfO_2 doped with BCP (HfO_2-BCP) was prepared as follows. Hafnium oxide was synthesized using hydrothermal method, and then was dispersed in the 1% solution BCP in ethanol. The resulting sol was deposited on the surface of QCR and dried at room temperature. As a reference sample for our measurements we used blank QCR, which surface is covered with gold electrodes. The latter are believed to play the major contribution in adsorption processes, compared with the surface of quartz.

Methodology of the measurements

Each of the samples, including reference sample, was placed in a gas-liquid cell and surface area of 5x5 μm was scanned three times in a row using Kelvin probe mode on the working QCR. Then the system was purged with air for 10 minutes (purge 1, fig. 2). After the air flow was turned off, again three scans were performed. Then, the system was purged with a gas mixture of target gas in air (10% ammonia or 0.1% hydrogen or 0,1% methane) for 20 min (purge 2, fig. 2), and six consecutive measurements of surface potential were performed in static atmosphere. Finally, the system was purged for 10 minutes with air (purge 3, fig. 2) and six scans were realized. After each scan the scanning direction was changed to the perpendicular one. The QCR frequency was measured continuously throughout the experiment. The color change upon injection of 10% NH3 in air was registered using built-in Solver ProM optical microscope.

Results and discussion

The change in the mass of the QCR was registered as a frequency change before and after exposition to the target gases, according to the (2). Table 1 shows the obtained results. First of all one should note that blank QCR seems to be not contributing significantly to the weight change upon analyte adsorption. In the case of NH_3 and H_2 exposition the highest adsorption capacity among all the materials manifests blank SnO_2. For CH_4 the highest change in the sample mass was observed for SnO_2-Pd. Note, that hydrogen adsorption for SnO_2 exceeds the one of CH_4, while for the Pd-doped material reverse tendency was found. Deposition of BCP apparently has little effect on the adsorption capacity of the target gases and does not increase it even in the case of NH_3. Comparing the gases, it becomes clear that NH_3, at concentration being 100 times higher than that of the rest target gases, adsorbs on the oxide surfaces in comparable quantity.

Table 1. The response of the QMB with the test materials to the effects of analyte.

Sample	The change in mass of the QCR, ng		
	10% NH_3 in air	0.1% H_2 in air	0.1% CH_4 in air
SnO_2	2198,2	1218,0	110,2
SnO_2(Pd)	333,5	no signal	203,0
BCP/HfO_2	43,5	2,9	2,9
QCR	8,7	no signal	no signal

The area on surface potential maps related only to the sample surface (fig. 2) was processed using software for image analysis Nova (NT-MDT). For each area, scanned one time, we found the average value of surface potential, corresponded to the maximum of the normal distribution function for the data array recorded during scanning. Such normalization of the obtained data was performed for each scan.

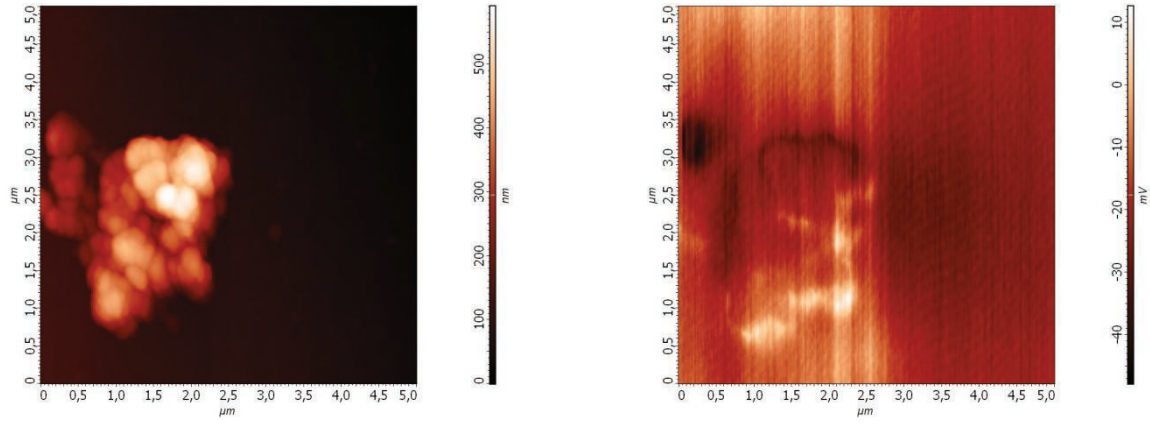

a b

Fig 2. Topography (a) and surface potential map (b) of the agglomerate of the particles on the surface of QCR in 10% NH_3 in air, sample SnO_2-Pd.

Fig. 3 shows the mean values of the measured surface potential for the experiment performed with 10% NH_3 in air. The highest change in surface potential upon introduction of ammonia vapors was

observed for blank SnO_2. However, for this material (as well as for blank QCR and HfO_2-BCP) the recovery of the surface potential is very slow at room temperature. Surprisingly, this was not the case of SnO_2-Pd, which manifested even at such low temperature full recovery of the surface potential after the sample was purged with air (purge 3). Fast recovery time of the surface potential was observed only in NH3 and only for SnO_2-Pd.

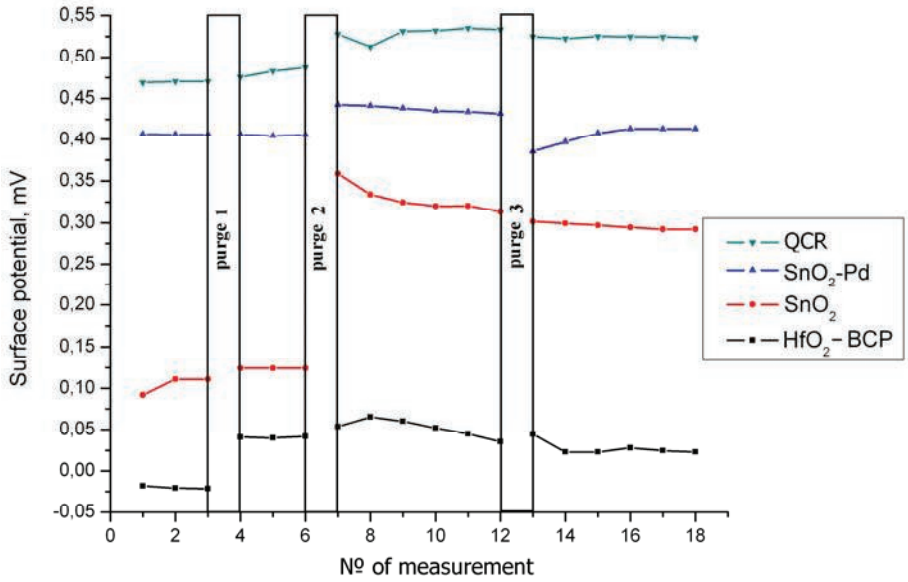

Fig. 3. The average values of surface potential of the samples when exposed to ammonia (purge 1 – air, purge 2 – 10% NH_3 in air, purge 3 - air).

Table 2 summarizes the results of the surface potential measurements for the analyte and materials in question. If we take into account the target gas concentrations, it becomes evident that all materials together with blank QCR manifest higher electronic related changes on the surface upon H_2 and CH_4 exposition, compared with NH_3 vapors. The highest potential change was found for blank material, which correlates with its high adsorption capacity. However note that for this material the highest potential change, found for CH_4, does not corresponds to the highest mass change found for H_2. This means that major part of the adsorbed H_2 does not form surface donor states under these experimental conditions.

Table 2.Change in surface potential of the materials in question upon different target gas adsorption

Sample	Change in surface potential, mV		
	10% NH_3 in air	0.1% H_2 in air	0.1% CH_4 in air
SnO_2	189,0	54,7	68,9
SnO_2-Pd	25,8	22,5	30,0
HfO_2-BCP	6,6	15,7	14,1
QCR	46,3	13,5	6,4

Reverse tendency is observed for SnO_2-Pd: while the mass change was not registered for this material upon H_2 exposition, the potential was changed. The same observations can be made for blank QCR. In the case of HfO_2-BCP, surface potential changes higher upon CH_4 exposition, compared to that of H_2. However, both analytes seem to be adsorbed in the amounts close to each other.

Conclusions

We realized *in-situ* simultaneous measurements of surface potential and mass of the adsorbed target gas using integrated SPM-QCR technique. Experimental applicability of the technique was demonstrated by example of adsorption of NH_3, H_2 and CH_4 on the surface of oxide materials. It was shown that the technique can be used to find correlations between the real amount of the adsorbed gases and the change of surface potential upon gas adsorption. The results demonstrate promising potentialities of the SPM-based techniques to study gas sensor properties of separate nanocrystals, measuring *in-situ* their surface potential. In addition, this technique allows simultaneously examine and most accurately compare sensor characteristics of the compact samples (particles or clusters) of several materials placed in the same scan area.

Acknowledgment

This work was partially supported by Presidium of Russian Academy of Science (project 8П3) and Russian Foundation for Basic Research (grant 10-03-01036). Also authors would like to thank E.N. Subcheva for assistance in carrying out the experiment.

References

[1] A. Oprea, N. Bârsan, U. Weimar, Work function changes in gas sensitive materials: Fundamentals and applications, Sensors and Actuators B: Chemical, 142 (2009) 470-493.
[2] E. Benes, M. Gröschl, W. Burger, M. Schmid, Sensors based on piezoelectric resonators, Sensors and Actuators A: Physical, 48 (1995) 1-21.
[3] F. Iwata, M. Kawaguchi, H. Aoyama, A. Sasaki, Ultrasonic micromachining on Al thin film using atomic force microscopy combined quartz crystal resonator, Thin Solid Films, 302 (1997) 122-126.
[4] F. Iwata, K. Saruta, A. Sasaki, In situ atomic force microscopy combined with a quartz-crystal microbalance study of Ag electrodeposition on Pt thin film, Applied Physics a-Materials Science & Processing, 66 (1998) S463-S466.
[5] D. Johannsmann, I. Reviakine, E. Rojas, M. Gallego, Effect of Sample Heterogeneity on the Interpretation of QCM(-D) Data: Comparison of Combined Quartz Crystal Microbalance/Atomic Force Microscopy Measurements with Finite Element Method Modeling, Analytical Chemistry, 80 (2008) 8891-8899.
[6] J.M. Kim, S.M. Chang, H. Muramatsu, Scanning localized viscoelastic image using a quartz crystal resonator combined with an atomic force microscopy, Applied Physics Letters, 74 (1999) 466-468.
[7] R.G. Pavelko, A.A. Vasiliev, E. Llobet, X. Vilanova, N. Barrabйs, F. Medina, V.G. Sevastyanov, Comparative study of nanocrystalline SnO2 materials for gas sensor application: Thermal stability and catalytic activity, Sensors and Actuators B: Chemical, 137 (2009) 637-643.
[8] V. Sevastyanov, D. Murashov, N.Kuznetsov, E. Simonenko, A. Vasiliev, Multicapillary quartz sensor cell with embedded nanocomposite receptors for optical detecting ammonia and amines, Conference OPTO 2006, Proceedings SENSOR+ TEST 2006, Nurnberg, Germany, 30 May-1 June 2006, 177-182.
[9] A.V. Shelaev, V.A. Bykov, Scanning probe microscope combined with tool for mass and dissipative properties measurement, Patent, in, Russian Federation, 2008.
[10] G.Z. Sauerbrey, Z. Phys. , 115 (1959) 206.
[11] H.O. Jacobs, H.F. Knapp, A. Stemmer, Practical aspects of Kelvin probe force microscopy, Rev. Sci. Instrum., 70 (1999) 1756-1760.